

Subsurface chemistry of mantles of interstellar dust grains in dark molecular cores

J. Kalvāns¹ and I. Shmeld²

¹ Institute of Astronomy, University of Latvia, Raina 19, Riga, Latvia
e-mail: kalvans@lu.lv

² Ventspils International Radioastronomy Centre of Ventspils University College, Inženieru iela 101, Ventspils, Latvia
e-mail: iivarss@venta.lv

Received February 3, 2010; accepted May 13, 2010

ABSTRACT

Context. The abundances of many observed compounds in interstellar molecular clouds still lack an explanation, despite extensive research that includes both gas and solid (dust-grain surface) phase reactions.

Aims. We aim to qualitatively prove the idea that a hydrogen-poor subsurface chemistry on interstellar grains is responsible for at least some of these chemical “anomalies”. This chemistry develops in the icy mantles when photodissociation reactions in the mantle release free hydrogen, which escapes the mantle via diffusion. This results in serious alterations of the chemical composition of the mantle because pores in the mantle provide surfaces for reactions in the new, hydrogen-poor environment.

Methods. We present a simple kinetic model, using existing astrochemical reaction databases. Gas phase, surface and subsurface pore reactions are included, as are physical transformations of molecules.

Results. Our model produces significantly higher abundances for various oxidized species than most other models. We also obtain quite good results for some individual species that have adequate reaction network. Thus, we consider that the hydrogen-poor mantle chemistry may indeed play a role in the chemical evolution of molecular clouds.

Conclusions. The significance of outward hydrogen diffusion has to be proved by further research. A huge number of solid phase reactions between many oxidized species is essential to obtain good, quantitative modeling results for a comparison with observations. We speculate that a variety of unobservable hydrogen-poor sulfur oxoacid derivatives may be responsible for the “disappearance” of sulfur in dark cloud cores.

Key words. ISM: abundances – ISM: clouds – Astrochemistry – Molecular processes

1. Introduction

It is widely accepted that molecular hydrogen and many other interstellar molecules form on interstellar dust grains. There has been wide research in the field of gas-grain chemistry occurring in the dark, dense cores of interstellar molecular clouds, including observations and calculations. Various desorption mechanisms and chemical reactions on the surfaces of the grains are investigated.

Several molecules in the interstellar medium at least are known whose abundances are not easily explained by gas-phase and grain surface-phase chemistry. These include OCS, HCN, SO, cyanopolynes, and others. In the warming star-formation regions there appear highly oxidized organic compounds that indicate that a different chemistry occurs in these regions or, as we believe, the ejection of heavily processed interstellar grain mantles into the gas phase.

The grain surface reactions in interstellar clouds by definition are subjected to heavy hydrogenation. The proper production of heavier and hydrogen-poor species is difficult to reproduce by calculations at least in some cases (Hasegawa & Herbst 1993a, van Weeren et al. 2009, Hatchell et al. 1998). We present an alternative explanation of this problem by considering the possibility that within the grain mantles below the surface layer there is a hydrogen-poor, chemically active material. The aim of this article is to qualitatively answer this question through existing knowledge and means of astrochemical problem solving.

There are only few such models that take into account more than one layer of the accreted species. There are some serious researches done which insist that the chemistry of the species frozen onto grains does not end with the formation of the next accreted layer. Shalabiea & Greenberg (1994) examine photon-induced processes inside the mantle. They conclude that photo-processing of grain mantles is the start of the synthesis of many species. Hasegawa & Herbst (1993b) use a 3-phase model to examine the formation and composition of the inner mantle. They found that radicals like OH, CH₃ etc. are absorbed into mantles in large numbers. We argue that the chemistry below the outer surface of the icy mantle has to be common and is an important path in interstellar molecule synthesis. Besides, they also note that grain surface reactions tend to overproduce hydrogenated species, which is the main problem we attempt to tackle in this work. Schutte & Greenberg (1991) examine the possibility of molecule desorption from the grains by chemical explosions within the grain mantle. Naturally, these reactions can be expected to alter the chemical composition of the mantle itself. Freund & Freund (2006) present a dust grain model based on the principle of solid solutions, producing results that explain important features in the molecular cloud composition.

We present a model of the processes on the surface and inside the “frozen” grain mantles with a basic concept that chemical reactions occur on the surface of pores (or cracks) inside the mantles. The point that makes the difference between the surface and mantle reactions is that the mantle is not directly exposed

to the ocean of hydrogen in a nebula, and thus a significantly different chemistry may develop. This gives an opportunity to present an explanation for some of the astrochemical mysteries. We do not use advanced calculation techniques or new reactions; we evaluate the importance of hydrogen diffusion through the grain mantle on the chemical composition of the mantles in dark molecular cloud cores. Thus, the model includes various physiochemical processes but otherwise keeps a rather conservative approach.

2. The model

2.1. Model considerations

Current models, e.g. Das et al. (2008), Goldsmith et al. (2008), van Weeren et al. (2009) insist that the collapse of an interstellar cloud to densities around 10^5cm^{-3} occurs at a time around 10^6 years and that molecules form simultaneously. Deposition onto grains proceeds at timescales comparable to cloud cooling and collapse, and most of the accreted matter will accumulate at late stages of the cloud evolution. Taking this into consideration we developed a steady-phase chemical model for timescales much longer than the cloud formation.

In order to investigate the molecular abundances in dark cloud cores under chemical equilibrium we used a chemical kinetics model with 352 molecules. The interstellar UV radiation (molecule photodissociation and photodesorption) has been neglected, the integration time was taken to be 10^{16}s , comparable to an interstellar cloud entire lifetime, and the cloud density $n_H = 10^5 \text{cm}^{-3}$. The gas temperature is taken to be 15K , the dust grain temperature – 10K . We used the UDFa06 dipole (*udfa06*) astrochemistry database (Woodall et al. 2006) is used to provide the gas-phase chemical reaction set. We adopted elemental abundances provided by Jenkins (2009). The elements permitted are H, He, C, N, O, Na, Mg, Si, S, Fe.

The grain chemistry is described in terms of surface reactions between species that are located on the outer grain surface or on a surface of pores inside the grain mantle itself. It might be possible to even more adequately describe the grain mantle chemistry with the concept of a solid solution or nanoporous matter. For the grain processes the surface reaction set by Hasegawa, Herbst, Leung 1992 and Hasegawa & Herbst (1993a) is used (neutral molecules only). Species without gas phase *udfa06* reactions were excluded from calculations, because they also lack the important photodissociation sink reactions (Sect. 2.6). These include N_2H , HOC , NaOH , etc. In order to provide a more adequate reaction set for each molecule, organic molecules are included up to C_5 only in the grain surface and mantle model. This is because larger molecules tend to have less surface reactions included, especially when one takes into account the number of atoms they contain. Notably, there is an almost complete lack of oxidation reactions for the more complex carbon species. These reactions are extremely important because our model shows that a highly oxidative environment is possible in the grain mantles.

Because of the use of a huge gas-phase reaction database and a limited solid-phase reaction database, there are many gas phase molecules that do not take part in the surface and mantle processes. Since our aim is to investigate exclusively the solid phase of interstellar molecules, we decided for the sake of completeness to leave the *udfa06* as intact as possible in our model, with some 260 gas-only species. Most of the molecules with a gas phase only are not relevant to the solid phase (ions), and the remainder are expected to have negligible abundances any-

way (complicated organic species). When one compares similar molecules with and without a solid phase, the difference in abundances is about one order of magnitude. The full list of results for gas-phase species is given in Table 4.

We used a chemical model integrated in a 3-phase system similar that of Hasegawa & Herbst (1993b). The three phases are gas, grain surface, and grain mantle. The grain surface consists of reactive species that accrete from gas, may be easily desorbed by several mechanisms, and are subjected to photodissociation. In this context the surface consists of the first few layers of a mantle. The mantle itself is formed by buried surface molecules. H atoms and especially H_2 molecules, which are created in the mantle by photolysis can migrate away from their parent molecule, and the mantle becomes enriched with free hydrogen. This excess hydrogen is can escape to the outer surface by diffusion. Thus, with photolysis a mostly hydrogen-poor chemical environment forms below the surface.

Molecules adsorbed onto grains are divided into two layers - the surface and the mantle. We employed a model of an equilibrium state, where surface and gas phase molecules are in a dynamic equilibrium, while mantle molecules are almost permanently locked away in a frozen state. Thus, “surface” represents a few (rugged) top layers that are subjected to desorption and surface reactions and may be brought to the very top layer by these processes. “Mantle”, by definition, is never exposed to the surface and is only slowly returned to the gas phase by direct ejection caused by cosmic ray hits. In order to properly describe the physical and chemical processes we avoided the division of the mantle in layers. Surface and mantle molecules are treated as solid species uniformly dispersed in volume with abundances expressed in cm^{-3} .

2.2. Molecule accretion onto grains

Molecule accretion onto grains happens in an equilibrium with the various desorption processes. In our model only neutral molecules accrete. The rate coefficient (s^{-1}) is calculated according to Willacy & Williams (1993) and Nejad & Wagenblast (1999) by the formula

$$k_{\text{accr}} = 3.2 \times 10^{-17} n_H S_i \left(\frac{T_g}{M_i} \right)^{1/2}, \quad (1)$$

where S_i is the sticking coefficient, M_i is molecular mass of species i in atomic mass units, and n_H is total number of H atoms per cm^3 , T_g is gas temperature (K).

The rate of accretion, $\text{cm}^{-3} \text{s}^{-1}$, is thus

$$R_{\text{accr}} = k_{\text{accr}} n_i, \quad (2)$$

where n_i is the gas phase abundance of species i .

The sticking coefficient used by previous authors (i.e. Willacy & Williams 1993, Nejad & Wagenblast 1999, Roberts et al. 2007, Aikawa et al. 1997, Turner 1998b, Willacy & Millar 1998, Brown & Charnley 1990) for heavy species is 0.1 to 1, usually around 0.33, and that for light species is 0 to 1. We took an approximate average path with $S_i=0.33$ for all heavy species and 0.1 for hydrogen atoms and H_2 molecules.

2.3. Thermal evaporation

The thermal evaporation rate is calculated from the evaporation times given in Hasegawa & Herbst (1993a).

2.4. Direct cosmic-ray heating desorption

Desorption by heating, caused by Fe nuclei of cosmic rays, is calculated with the rate coefficients given by Hasegawa & Herbst (1993a).

2.5. Cosmic ray induced photodesorption

Rate coefficient (s^{-1}) for desorption by cosmic ray induced photons for surface species is calculated by the formula adapted from Willacy, Williams (1993)

$$k_{crpd} = R_{ph} Y, \quad (3)$$

where the photon hit rate R_{ph} for a single grain

$$R_{ph} = F_p \langle \pi \alpha_g^2 \rangle. \quad (4)$$

Yield Y is taken to be 0.1, F_p is photon flux, taken $4875 \text{ cm}^{-2} \text{ s}^{-1}$ from Roberts et al. (2007). $\langle \pi \alpha_g^2 \rangle$ is the average cross section of a grain ($1.0 \times 10^{-10} \text{ cm}^2$). Like for other desorption mechanisms, the desorption rate is

$$R_{crpd} = k_{crpd} n_{surf,i}. \quad (5)$$

$n_{surf,i}$ is the average abundance (cm^{-3}) of species i residing on the outer surface of a grain.

2.6. Dissociation by cosmic ray induced photons in solid state

Besides the surface binary reactions of Hasegawa, Herbst, Leung, (1992) and Hasegawa & Herbst (1993a), we also include a limited set of cosmic ray photon induced photoreactions on grain surfaces.

We pretend that the individual molecules on and in the amorphous mantles with mixed composition essentially keep their UV absorption properties. The gas phase reaction coefficients we obtain from *udfa06*. H and H_2 formed in photodissociation on the outer surface of grains are always allowed to escape into gas phase, while all other species remain on the grain surfaces (their desorption by CR induced photons is described above in Sect. 2.5). We consider it a reasonable approximation given that the surface species in the model of Hasegawa & Herbst (1993b) are probably too intensively hydrogenated, and Andersson & van Dishoeck (2008) concludes that photodissociation of amorphous water ice mostly results in an escaping hydrogen atom.

Several sources (Shalabiea & Greenberg 1994, Andersson & van Dishoeck 2008, Öberg et al. 2009) indicate that photoreactions can and do occur in the layers below the surface, although they usually do not lead to desorption.

Thus, the formula for photodissociation rate coefficient is

$$k_{ph.dis} = k_{udfa} Y_{dis}. \quad (6)$$

Generally, the quantum yield is taken to be 0.1 for any given species on grain surface $Y_{s.dis}$. We assume that within the mantle only molecules with access to a surface can be effectively dissociated, so that the products do not recombine again. We expect 1/100 of the mantle to be exposed to inner pore surfaces. The dissociation yield for mantle molecules is

$$Y_{mantle.dis} = 0.1 \times 10^{-2}.$$

The dissociation products of these inert molecules are then assumed to be reactive until they become frozen again (see Sect. 2.8).

2.7. Desorption resulting from H_2 formation

We calculated the rate coefficient (s^{-1}) for desorption of surface molecules by heat released by H_2 molecule formation on grains according to Roberts et al. (2007)

$$k_{\text{Hf.des}} = \frac{\epsilon R_{\text{H}_2}}{n_g}, \quad (7)$$

where the abundance n_g (cm^{-3}) of dust grains is

$$n_g = 1.33 \times 10^{-12} \times n_H. \quad (8)$$

R_{H_2} is the formation rate of H_2 molecules and ϵ is number of molecules desorbed per act of H_2 molecule formation. The species desorbed are those with binding energies E_b below a threshold energy. According to the discussion by Willacy & Millar (1998) and Roberts et al. (2007), the efficiency of desorption by heat released by H_2 formation is a subject of discussion and suggestions. Following Roberts et al. (2007) we take $\epsilon=0.01$. Like in other models, this selective desorption mechanism has a strong effect on the abundances of major species in both, gas and solid phases. We choose to diminish its importance by taking $E_b < 1210\text{K}$ (binding energies from Hasegawa & Herbst 1993a).

2.8. Binary reactions on grains

For chemical processes on grain surfaces, i.e. reactions between accreted species, we use the reaction set provided by Hasegawa, Herbst & Leung (1992) and Hasegawa & Herbst (1993a). The rate coefficient is

$$k_{ij} = \frac{\kappa_{ij}(R_{diff,i} + R_{diff,j})}{n_g}, \quad (9)$$

where the diffusion rate is

$$R_{diff} = N_s^{-1} \times t_{hop}^{-1}. \quad (10)$$

Because the roughness and inhomogeneity of the mantle are key features of this model, we used the higher quantity 2×10^6 for number surface adsorption sites N_s instead of 10^6 , which characterizes a perfect spherical grain. κ_{ij} is the probability for the reaction to happen upon an encounter, t_{hop} is the hopping time (s) for mobile species.

We assume that physical transformations of a fully formed grain mantle in steady conditions inside dark cores are driven by cosmic rays passing through the grain. When a heavy cosmic ray particle hits the grain, the mantle is heated, shaken, and at least locally rearranged. New surfaces appear and molecules and some radicals emerge, migrate, and react, while other species become locked in ice again. Thus the mantle (and, perhaps, the grain) is not a frozen chunk of molecules but undergoes changes in timescales comparable to cloud lifetimes. Generally, reactions occurring within the icy mantles should be of great importance because most of the frozen molecules are accumulated in the volume, not the surface. Cosmic-ray-induced alternations are generally regarded as first-order reactions. We keep this approach here. Molecules in a mantle are activated with a rate coefficient (s^{-1})

$$k_{act} = t_{cr}^{-1} \times u^{-1}, \quad (11)$$

where t_{cr} is the average time between two successive strikes by a Fe cosmic ray nucleus (calculated $3.16 \times 10^{13} \text{ s}$ by Hasegawa & Herbst 1993a) and u is the number of strikes needed to fully

reorganize the grain mantle, i.e. to expose to an inner surface an amount of molecules equivalent to the total number of molecules per mantle. u is dependent on the porousness and thickness of an average mantle. The thickness is estimated to be 100 monolayers by Hasegawa & Herbst (1993b) and 25 layers by Turner (1998a). The former value is generally more consistent with our model. We assumed $u=200$.

The reactions of the activated (exposed to a pore surface) reactants proceed with the rate coefficient (Hasegawa, Herbst & Leung 1992)

$$k_{mantle,ij} = \frac{\kappa_{ij}(R_{diff,i} + R_{diff,j})}{n_g n_p}. \quad (12)$$

There is no knowledge about pores of interstellar dust; their size and numbers should be affected by the exact conditions in the dark core. However, they are limited by the number of mantle layers and size of the grain (see above). Undoubtedly, most of the pores are too small to provide a functioning reaction surface, while there should be only a few larger pores and with a higher possibility to be connected to the outside, thus indeed becoming at least partially a gully of the outer surface. For the calculation of the diffusion rate R_{diff} the number of adsorption sites per average pore N_s in Eq. 10 is now taken to be 10^3 . We take the same number for the pores per grain, $n_p = 10^3$. We consider this choice a possibly neutral estimate.

The factor that changes the reaction rate taken from Hasegawa, Herbst & Leung (1992) and Hasegawa & Herbst (1993a) is inversely the number of isolated surfaces in a grain multiplied by the number of adsorption sites on the available surface. For outer surface (as given in Hasegawa, Herbst & Leung 1992, Eqs. 4 and 9) this factor is

$$\frac{1}{1 \times 10^6 \times n_g}.$$

For pores we take

$$\frac{1}{10^3 \times 10^3 \times n_g}.$$

That is, we assume that there are thousand pores in an average grain with a surface of thousand adsorption sites each.

The molecules are assumed to be in the activated state from a Fe cosmic ray hit to about the time of the next cosmic ray hit. The interval of hits is assumed to be t_{cr} (s). The rate coefficient (s^{-1}) is thus

$$k_{inact} = t_{cr}^{-1}. \quad (13)$$

The chosen rate coefficients ensure that at any given time instant roughly 0.5% of mantle species are “activated” and are taking part in reactions on the pore surfaces. It is half the number of molecules assumed to be exposed to pore surface. The remaining half is assumed to be inactive for some reason (molecules which reside in pores too small for reactions and temporarily blocked sites). The molecular abundances (gas, surface, and mantle) produced by the model are only very slightly dependent on this percentage. It is because the chemical reactions on surface are anyway much faster than the radical production on surfaces by CR induced photons.

2.9. Hydrogen diffusion through mantle

Hydrogen diffusion from the surface to the mantle pores and from the mantle to the surface is included in our model. We

calculated the diffusion rate coefficient assuming that H atoms and H_2 molecules mostly reside on outer or inner surfaces. The hydrogen within the mantle lattice is only a relatively rare intermediate state. Thus

$$k_{H,diff} = DP_{diff}L, \quad (14)$$

where D is the diffusion coefficient, P_{diff} is the probability for diffusing species to find an appropriate surface. L is the length of the diffusion path (we take it $1 \times 10^{-6}cm$), approximately half the thickness of the mantle. We adopt D for H atoms $2.50 \times 10^{-21}cm^2s^{-1}$ estimated by Awad et al. (2005). For the H_2 molecules we use the coefficient given by Strauss & Chen (1994) for diffusion in hexagonal ice extrapolated to 10K ($D_{H_2} = 5.90 \times 10^{-8}cm^2s^{-1}$). This may sound rather tentative as the diffusion in amorphous ice is expected to be significantly slower. We could not find any estimates for D_{H_2} in amorphous ice, however, in our model the real hydrogen content is rather independent of the exact value of D_{H_2} as long as $D_{H_2} \gg D_H$ and the real H_2 diffusion rate is much shorter than the photodissociation rate – both of which are expected to be true.

We use the value $P_{diff,MS}=0.5$ for outward diffusion (assuming that on average 50% of all diffusion directions from pores lead outwards) and $P_{diff,SM} = 1 \times 10^{-2}$ for inward diffusion because in our model we expect only 1/100 of the mantle volume to be occupied by the larger pores, able to host enough reactants on their surfaces for reactions to occur. This means that 99% of surface hydrogen diffusing inward returns to the surface and only 1% reach an inner pore to reside in. These probabilities result in an equilibrium where the outward flux of hydrogen dominates. A release of hydrogen and the formation of less hydrogenated species is observed in numerous experiments involving photolysis of hydrogenated species in vacuum, e.g. Gerakines et al. (1996), Andersson & van Dishoeck (2008).

2.10. Direct ejection by cosmic rays of mantle molecules

Certainly there must be a process besides the transfer of gas molecules to the surface and then to the mantle that works in the opposite direction or a complete freeze-out will result, which is not observed. We propose a simple cosmic-ray-driven mechanism which consistently returns a proportion of the inner mantle into the gas phase. These are the molecules believed to be directly, unselectively ejected by a hit of a Fe cosmic ray nucleus. The rate of ejection ($cm^{-3}s^{-1}$) is calculated by

$$R_{ej} = t_{cr}^{-1} Y_{cr} n_g X_{mantle,i}. \quad (15)$$

$X_{mantle,i}$ is the proportion of species i in the grain mantle. Y_{cr} is the number of mantle molecules ejected by this process in each hit. It should be a negligible number compared to the number of molecules desorbed by the cosmic-ray heating mechanism, estimated to be at least 10^6 by Hasegawa & Herbst (1993a). We take Y_{cr} 0.01% of this value, that is 100 molecules per hit of cosmic-ray Fe nuclei. Gas and solid phase abundances are unaffected by the value of Y_{cr} over several orders of magnitude. The returning of mantle molecules into the gas means that gas, surface, and mantle phases are in an interconnected equilibrium in our model. Molecule abundances in both surface and mantle directly affect the abundances in gas, where the species are easily observable.

2.11. Surface-to-mantle transition

We calculated the transformation of the surface species into mantle species in the local thermodynamic equilibrium with a constant rate coefficient

$$R_{\text{mantle}} = k_{\text{circ}} n_{\text{surf},i}. \quad (16)$$

k_{circ} is the total circulation rate of a surface molecule at an equilibrium state. The molecule accretes from the gas phase, undergoes surface diffusion, reactions, desorption acts, and is eventually buried by other molecules, and finally ends up in the mantle. We treat this coefficient as an unknown variable and use the model with the given, often assumed, input conditions (Sect. 2.2 to 2.5 and 2.7, and 2.10) to choose k_{circ} . We took $3.7 \times 10^{-17} \text{ s}^{-1}$ to produce a ratio 30:1 between the total abundances of all atoms in the mantle and on the surface (except hydrogen). Gas, surface, and mantle abundances are very strongly affected by the value of k_{circ} , consequently it has to be chosen with a precision to decimals. H and H₂ are not incorporated into the mantle by this mechanism.

It is not a physically adequate approach to calculate the rate of surface-to-mantle transition. However, with so many assumptions and poorly known values used (e.g. S_i , Y_{cr} , u etc.) we consider it satisfactory for the aims of this paper. This approach also implies that the program might produce somewhat biased results in terms of absolute abundances (cm^{-3}).

2.12. Desorption by chemical explosions

We do not include desorption by chemical explosions (Schutte, Greenberg 1991) of grain mantles. In our current model the radicals released by photoprocess do not react rapidly and violently as is required by the explosion theory. They are entirely consumed by the reactions on the pore surfaces. Less than 1/100 of the mantle species are radicals in calculation results of our model, partially due to the incomplete reaction network. However, the photon flux in dark cores is significantly lower than in experiments producing explosion effects. Fully researching them requires a more sophisticated model, because the explosive reactions also directly affect the chemical composition of the icy mantle.

2.13. Model credibility

To focus our research on chemical processes at the local thermodynamic equilibrium we investigated a standard case of a very long-existing interstellar dark cloud core, completely isolated from the interstellar UV radiation field. The parameters regarding the various physical and chemical transformations of solid phase species (Sect. 2.1 - 2.11) were chosen in accordance with our understanding of the grain structure and processes. These parameters are able to influence the model output (calculated fractional abundances) in a wide range.

Observational results found in the literature were used to evaluate the rate of ejection of the mantle molecules by cosmic rays (Sect. 2.10) and surface-to-mantle transition (Sect. 2.11). These two rates essentially determine the abundances of gas phase species. We opted for long-lived (presumably LTE) interstellar cloud cores – dark, cold, and with metals heavily depleted on grains (Hollenbach et al. 2009, Turner 2000, Tafalla et al. 2004).

There are several aspects or assumptions in the model that require a credibility assessment. Most important is, how close

the pore surface model represents the real conditions on interstellar grain mantles. Under certain (given) input conditions the model can produce feasible results. We assume that small pores are insignificant for the mantle chemistry, but they may affect the hydrogen content within the mantle to an unknown extent. Also, we do not take into account the ability of hydrogen to react while diffusing through the solid amorphous ice. Generally these effects should lead to an increased abundance of hydrogenated species at the expense of radicals (perhaps reducing the efficiency of desorption by explosions).

A second aspect regarding the validity of the model is the yields of various photoprocesses, especially the yield of the photodissociation inside the mantle. The model works best with the assumption that below the few surface layers dissociation essentially occurs on pore surfaces only. This is certainly not true, as dissociation basically is not a surface-related process. However, the assumption is justified by the higher possibility of recombination of dissociation products unable to diffuse away in a (amorphous) lattice. However, some the hydrogen released within the lattice may be able to diffuse, again increasing the radical content and supplying atomic hydrogen for reactions and diffusion to the surface. Si, Na, Mg and Fe have a very limited or nonexistent set of solid phase reactions and species and we do not include these elements in our discussion about results. Silicon is kept in the surface-mantle model in order to increase the total number of available reactions and thus improve the general accuracy of results for other species.

3. Results

We recall here that the simplified approach in the model is a quick solution to promote the discussion about the importance of hydrogen diffusion effects on grain mantle chemical composition. We emphasize that an important feature is the limited number of reactions available for each species in the mantle. A typical solid heavy molecule, for example, C₅H₂ or SO, has one or two dissociation reactions by cosmic ray photons. Also, there are usually two to three reactions where the species is a product. There are usually no more than six reactions (production and destruction) involving a complicated molecule. It is a poor set of chemical transformations, especially in the mantles where hydrogenation reactions play a role of relatively little importance. Thus the calculated abundances for several important species are highly biased, as noted below.

The calculation results are summarised in Tables 1, 2, and 3 and in Fig. 1.

The overall results of the model are shown in Table 1. Results (Table 2) show that the mantle-to-surface (M/S) ratios for heavy elements are different from each other. This means that, for example, M/S of C₅ and O₂ molecules is not directly comparable, because the M/S ratio of carbon itself is higher than that of oxygen (cf. Table 2) and there is a larger abundance of carbon species overall in the mantle. To be able to compare the mantle-to-surface ratios of different molecules, we calculate a weighed average elemental M/S ratio (WR) for each individual specie according to

$$WR_m = \frac{\sum_j^i (a \times RE)}{\sum_j^i a}. \quad (17)$$

a (the index in a molecular formula) is the number of atoms of elements i to j in the molecule m . RE is the average M/S ratio for each element in the molecule m (C, N, O, Na, Mg, Si, S or

Fe) from i through j . Because hydrogen wanders rather freely between the surface and the mantle, it is not counted here. We name the relation

$$\frac{(M/S)_m}{WR_m} \quad (18)$$

the normalized mantle-to-surface ratio (nM/S). For species whose fractional abundance is equal in the mantle and on the surface, nM/S is unity. If the concentration in mantle is higher this value is higher than unity and vice versa. The nM/S for selected species are graphically shown in Fig. 1.

The cosmic-ray-induced photodissociation yield in lower mantle layers should be rather low, because with yields larger than 10^{-3} in our simulations we obtain a mixture of compounds with water not the dominant molecule, which is inconsistent with the present knowledge about interstellar grain mantle composition. In this case the remaining oxygen is lost mostly to highly oxidized carbon-bearing species.

Hydrogen in its atomic, molecular, and chemically bound states is a special case because it is the only element capable of crossing the boundary between mantle and surface (Sect. 2.9). The data regarding “solid” phases of H are shown in Table 3. As a standard comparison data for this paper (Table 1) we use the results given by Hasegawa & Herbst (1993b), Table 1, $t=1.0E+8$ yr. To properly compare the results we also calculated the molecular nM/S ratios for these data. Both works aim to investigate the solid phase chemistry in molecular clouds, and both have a 3-phase system (gas, surface, mantle). There are several important differences between the two models. Our model includes a reduced number of solid state species (see Sect. 2.1). The model of Hasegawa & Herbst lacks cosmic-ray-induced photodissociation of solid state species (Sect. 2.6), mantle-phase reactions (Sect. 2.8) and hydrogen diffusion (Sect. 2.9).

The main difference in the chemical modeling results is that we obtain more oxidized compounds, like H_2O_2 in the mantle. They are mainly CO_2 , $HCOOH$ and less CH_4 for carbon, SO_2 for sulfur, more HCN , N_2 and less NH_3 for nitrogen. Generally one can say the improvements of our solid phase model diminishes the dominance of hydrogenated species and leads to a much greater chemical diversity with high abundances of fully or partially oxidized species. Another substantial difference in our model is the high concentration of atomic and other radical species, both on the surface and in the mantle. It can be attributed to the inclusion of photodissociation reactions for all solid species. Our model produces a much better overall fit to observations for gas phase species. It is because molecules dominant in the mantle phase are slowly returned into gas and partially reprocessed, and a total freeze-out for any species cannot occur.

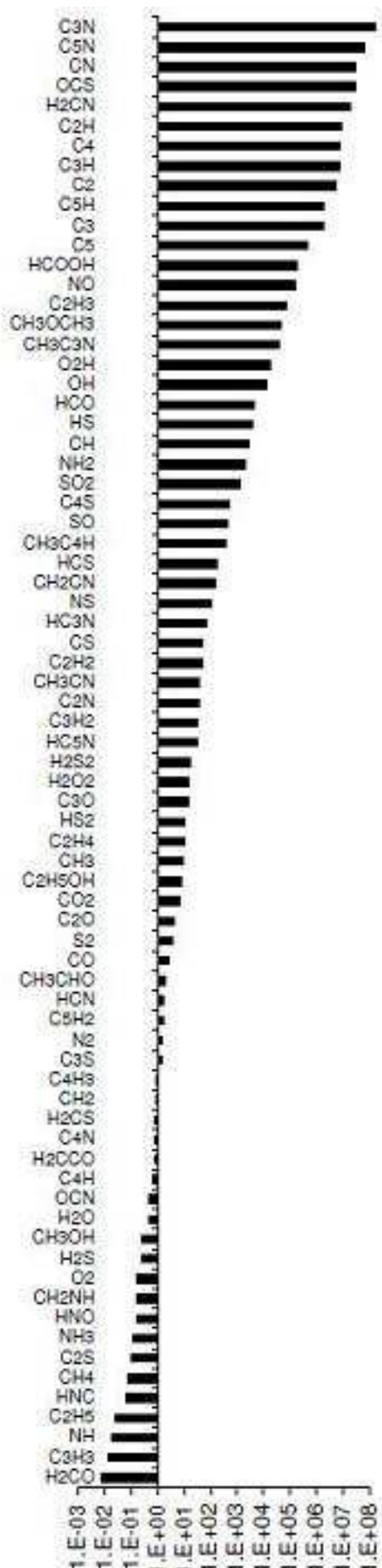


Fig. 1. The normalized mantle-to-surface (nM/S) ratio for selected species, obtained from Table 1 data.

Table 1. Calculated fractional abundances of species in gas, surface, and mantle phases, and the normalized mantle-to-surface ratio. Included species are with both gas and solid phases only.

Species	Gas	Surface	Mantle	nM/S	Species	Gas	Surface	Mantle	nM/S
C	4.56E-09	1.32E-17	2.15E-14	4.62E+01	OCS	2.99E-10	1.54E-16	1.58E-07	2.84E+07
N	1.52E-08	1.25E-14	2.59E-14	6.78E-02	SO2	3.09E-12	1.37E-10	5.99E-06	1.25E+03
O	8.83E-08	7.44E-17	2.35E-14	1.01E+01	CH3	1.48E-08	2.82E-14	9.05E-12	9.14E+00
NA	4.71E-09	8.23E-08	2.90E-06	1.00E+00	NH3	5.81E-08	8.34E-08	2.94E-07	1.15E-01
MG	1.18E-07	2.01E-06	6.78E-05	1.00E+00	SIH3	3.08E-09	1.44E-14	3.08E-07	9.71E+05
SI	1.79E-08	1.21E-14	3.05E-07	1.15E+06	C2H2	3.72E-09	1.08E-08	1.94E-05	5.10E+01
S	1.88E-08	1.52E-14	7.44E-07	1.15E+06	H2O2	1.08E-08	1.60E-07	7.18E-05	1.43E+01
FE	1.62E-07	1.81E-06	5.61E-05	1.00E+00	H2S2	5.71E-11	5.82E-10	4.47E-07	1.81E+01
CH	6.73E-09	7.95E-20	7.81E-15	2.79E+03	H2CN	9.53E-12	1.27E-20	7.59E-12	1.82E+07
NH	2.37E-08	3.32E-14	1.92E-14	1.89E-02	H2CO	7.70E-08	7.21E-06	1.69E-06	7.03E-03
OH	3.79E-07	3.92E-13	1.61E-07	1.31E+04	C3H	1.22E-09	2.27E-15	5.35E-07	6.72E+06
C2	1.54E-09	1.14E-15	2.26E-07	5.63E+06	H2CS	3.50E-09	8.21E-08	2.64E-06	8.29E-01
CN	9.49E-09	2.14E-15	2.00E-06	2.84E+07	C4	9.91E-11	1.30E-16	3.47E-08	7.57E+06
N2	2.32E-08	3.31E-07	1.42E-05	1.40E+00	C3N	2.31E-11	3.36E-17	2.93E-07	2.56E+08
CO	3.92E-07	1.96E-07	1.73E-05	2.66E+00	C3O	3.06E-11	7.57E-10	3.65E-07	1.41E+01
SIH	5.05E-10	1.24E-14	2.92E-07	1.07E+06	C3S	1.49E-10	1.45E-09	7.24E-08	1.35E+00
NO	8.11E-08	4.12E-13	1.85E-06	1.45E+05	CH4	5.68E-08	1.74E-06	4.68E-06	7.65E-02
O2	7.34E-08	5.25E-08	2.73E-07	1.66E-01	SIH4	6.29E-08	1.29E-06	3.68E-05	1.29E+00
HS	8.58E-09	3.61E-12	6.15E-07	4.02E+03	C2H3	1.60E-10	9.65E-15	2.24E-08	6.60E+04
SIC	6.74E-10	8.84E-09	2.33E-07	9.21E-01	CH2NH	1.43E-08	2.14E-07	1.15E-06	1.63E-01
SIO	1.33E-07	1.65E-06	2.67E-05	6.05E-01	C3H2	2.60E-09	5.56E-09	6.28E-06	3.22E+01
CS	2.61E-09	5.35E-10	1.06E-06	5.13E+01	CH2CN	9.68E-11	1.29E-09	6.70E-06	1.54E+02
NS	2.04E-09	1.28E-10	5.33E-07	1.14E+02	H2CCO	5.20E-10	6.48E-09	1.70E-07	7.75E-01
SO	1.81E-11	9.27E-11	1.46E-06	4.28E+02	HCOOH	1.07E-12	1.31E-11	7.17E-05	1.68E+05
SIS	1.77E-15	1.87E-14	1.88E-07	3.12E+05	C4H	1.84E-09	1.56E-08	3.66E-07	6.66E-01
S2	2.22E-09	2.32E-08	3.74E-06	3.81E+00	HC3N	3.88E-10	5.16E-09	1.28E-05	7.31E+01
CH2	6.19E-09	1.44E-15	4.31E-14	8.52E-01	C5	9.15E-10	3.91E-16	6.25E-09	4.55E+05
NH2	7.30E-08	9.41E-14	6.08E-09	2.11E+03	C4N	2.47E-10	2.54E-09	7.15E-08	8.21E-01
H2O	2.84E-07	1.70E-05	2.42E-04	4.53E-01	C4S	3.17E-13	2.86E-12	5.18E-08	4.94E+02
SIH2	2.82E-10	1.25E-14	3.05E-07	1.10E+06	CH2H4	8.64E-09	1.03E-09	3.73E-07	1.03E+01
C2H	6.91E-09	5.95E-15	1.72E-06	8.23E+06	CH3OH	2.58E-10	3.41E-09	3.05E-08	2.69E-01
O2H	5.08E-13	4.45E-14	2.63E-08	1.88E+04	C3H3	3.76E-09	1.20E-07	5.88E-08	1.40E-02
HS2	1.10E-10	1.14E-09	5.38E-07	1.11E+01	CH3CN	4.06E-11	4.71E-10	5.88E-07	3.71E+01
HCN	3.86E-08	9.45E-07	5.33E-05	1.71E+00	C5H	2.08E-10	6.81E-16	4.28E-08	1.79E+06
HNC	2.05E-08	3.07E-07	7.01E-07	6.94E-02	C5N	2.56E-11	1.10E-17	2.46E-08	6.48E+07
HCO	8.30E-09	4.53E-13	6.64E-08	4.41E+03	C2H5	4.76E-09	4.10E-07	3.77E-07	2.62E-02
HCS	5.96E-10	1.70E-15	1.08E-11	1.64E+02	C4H3	1.77E-09	2.07E-08	6.64E-07	9.11E-01
HNO	1.44E-08	1.44E-06	6.90E-06	1.55E-01	CH3CHO	1.26E-09	1.54E-08	9.53E-07	1.83E+00
H2S	8.06E-09	5.49E-07	6.25E-06	2.68E-01	C5H2	6.09E-10	2.30E-08	1.26E-06	1.55E+00
C3	1.59E-09	8.85E-16	5.29E-08	1.70E+06	HC5N	4.17E-11	6.21E-10	6.87E-07	3.22E+01
C2N	2.16E-10	2.24E-09	2.66E-06	3.53E+01	CH3C3N	1.72E-14	1.72E-13	2.41E-07	4.08E+04
C2O	2.06E-10	2.12E-09	3.28E-07	4.57E+00	CH3OCH3	2.38E-15	2.79E-14	3.92E-08	4.15E+04
C2S	5.84E-10	6.07E-09	2.35E-08	1.03E-01	C2H5OH	4.69E-13	5.16E-12	1.38E-09	7.87E+00
OCN	4.80E-08	4.75E-07	7.81E-06	5.08E-01	CH3C4H	3.93E-13	3.94E-12	5.15E-08	3.72E+02
CO2	3.89E-08	6.92E-07	1.64E-04	7.26E+00					

Table 2. Total elemental fractional abundances in surface and mantle phases, calculated from Table 1 data.

Element	Surface	Mantle	Mantle-to-surface
C	1.35E-05	4.73E-04	3.51E+01
N	4.14E-06	1.27E-04	3.07E+01
O	2.98E-05	9.35E-04	3.14E+01
Na	8.23E-08	2.90E-06	3.53E+01
Mg	2.01E-06	6.78E-05	3.38E+01
Si	2.95E-06	6.50E-05	2.20E+01
S	6.89E-07	2.93E-05	4.24E+01
Fe	1.81E-06	5.61E-05	3.10E+01

Table 3. Fractional abundances for hydrogen species in surface and mantle phases.

Species	Surface	Mantle	Mantle-to-surface
H ₂	1.17E-05	2.34E-07	2.00E-02
H	1.25E-18	2.17E-20	1.73E-02
H (chemically bound)	6.84E-05	1.12E-03	1.64E+01

The main results of our investigation are:

1. Important molecules on the surface are H₂O, H₂CO, CH₄. Those in the mantle are H₂O, CO₂, HCOOH, H₂O₂ (Table 1). The most abundant molecule among both the surface and mantle species is water. However, the molecule containing most of the oxygen in the mantle is CO₂. In our opinion this represents the general shift from highly to poorly hydrogenated species by the photochemical processing of the mantle.
2. The nM/S ratio for highly hydrogenated species is usually rather low, in the range 0.1 - 0.01 (Fig. 1). The most important species here are CH₄ and other saturated carbon molecules. Methane has a high concentration on the surface, which significantly decreases in the mantle, releasing huge amounts of carbon now available for various oxidized and chain-like compounds.
3. The highest nM/S is seen for cyanopolyne related molecules, showing that mantle processing efficiently transforms saturated hydrocarbons to these species. The related HNC is consumed in the mantle, and the HCN/HNC gas abundance ratio of 1.9 is adequate for dark cores. Remarkable are the high nM/S values for oxidized sulfur species (OCS, SO, SO₂), although these molecules have a very limited reaction set. The abundance of S oxides in the mantle exceeds that of H₂S. We expect that hydrogen depletion in the mantle should essentially explain the high abundance of OCS and sulfur oxides in hot core regions noted by many observers (e.g. Mookerjea et al. 2007, Hatchell et al. 1998). We predict that 3-phase models with a more complete reaction network will produce OCS and other sulfur species in an amount more consistent with the observations.
4. According to calculations, the hydrogen depletion in the mantle has different effects on the abundances of carbon-oxygen compounds. Molecules HCOOH and HCO have large nM/S, for C₃O, C₂O, CH₃CHO it is mediocre, and for CH₃OH, H₂CO nM/S is less than unity. With a limited degree of certainty one can conclude that weakly hydrogenated C-O species are those favored by the conditions inside grain mantles, which is confirmed by observations of hot cores (e.g. Mookerjea et al. 2007). Molecules CH₃OCH₃, C₂H₅OH and H₂CCO have a very deficient chemical reaction set and are not considered here.
5. An increased radical content in the mantle. Species like C, O, CH, S and others (notably excluding nitrogen species) show nM/S ratios moderately higher than 1. The model-based explanation is that only a limited reaction network is available and that not all species produced by the dissociation of CR induced photons are able to readily react and generate stable molecules. However, the real radical content depends on photodissociation yields and on the exact conditions in the mantle (see Sect. 2.13).

4. Discussion

There is some experimental evidence available in the literature that backs up the results. Ferrante et al. (2008) and Garozzo et al. (2010) show experimentally that OCS is readily formed in laboratory-simulated interstellar conditions, while our model shows OCS to be a molecule with a very high nM/S ratio. However, we note again that OCS has a very limited reaction set. Several sources (e.g. Weaver et al. 2005 and references therein) note high abundances of organic molecules with H, C and O in regions of grain mantle disruption or evaporation, indicating that these species are formed on grains. This agrees with our model results, where most of these species have nM/S higher (much higher for some molecules) than unity (Fig. 1).

Our model shows that the hydrogen diffusion outwards from the mantle is much more significant than the inward diffusion. The species initially included in the mantle are hydrogen-rich due to the surface reactions. Photoprocessing releases the chemically bound hydrogen, it diffuses, escapes to the surface and, eventually, the gas phase. According to the model, this process is not overcome by the hydrogen diffusing into the mantle from outside.

Although the hydrogen diffusion coefficient in amorphous, dirty ice is most probably smaller than the one we used (in hexagonal ice), the model is insensitive to the exact value of D over several orders of magnitude. This is the case as long as the time of the diffusion is much shorter than the heavy molecule residing time in the mantle. Also, the model is rather insensitive to the exact value of inward diffusion probability $P_{diff,SM}$, if it is kept lower (for example, by a factor of 2/3) than the outward $P_{diff,MS}=0.5$. The solid phase model results are essentially determined by the reasonable estimate (see Sect. 2.9) that $P_{diff,MS} > P_{diff,SM}$. With a degree of certainty one can say that the total direction of hydrogen diffusion at 10K (in, immobile, or out) is determined by the structure of the mantle, not by the exact diffusion speed.

The hydrogen atoms released in mantle photodissociation are very slow to diffuse and are very reactive. However, among other molecules, there always form H₂ molecules that are generally much less reactive and able to easily diffuse and leave the mantle. While hydrogen is depleted, methane and other highly saturated hydrocarbons transform to cyanopolyynes and other hydrogen-poor carbon chain compounds (Fig. 1). Water slowly loses hydrogen and the remaining oxygen forms compounds with other metals (in our model it is mostly CO₂).

The most serious counter-argument produced by our model is the overabundance of the CO₂ molecule in calculation results. However, like many others, this important species is badly affected by a poor reaction set, its only sink reaction is the slow dissociation by cosmic-ray-induced photons. This is also the exact reason why chains with six and more carbon atoms were excluded from our calculations. The concentration of overproduced molecules would be reduced by interaction with radicals

(including atomic hydrogen) in the mantle, meanwhile reducing the amount of radicals themselves. In the reaction set by Hasegawa, Herbst & Leung (1992) and Hasegawa & Herbst (1993a) most important radicals that lack solid phase reactions have the general formula MH_x where M is C, N, O, S or Si. They are generated by photodissociation in our model. The reactions between any complicated species and a variety of radicals are desirable for future mantle chemical models.

The differences in elemental abundance within mantle and surface (Table 2) can be clearly accounted for selective desorption effects by direct cosmic-ray-heating and by H_2 formation. Carbon is accumulated because it tends to form chain-like heavy molecules, while sulfur molecules generally have high binding energies and also do not easily desorb.

The hydrogen-poor conditions within the grain mantles may promote a much more colorful chemistry than is usually thought about interstellar matter. In the model it can be seen best with the C-O compounds. Reasoning from the calculation results we expect that the sub-surface mantle conditions would favor an assortment of (1) rather complex and (2) oxidized species. If we attribute these properties to the heavier elements, we can conclude that a significant proportion of Si, P, and S should be highly oxidized and in molecules forming many bonds. Strong inorganic or semi-organic acids, their salts and esters with the organic alcohols, peroxy acids, etc., can be some of the compounds whose formation can be permitted by the lack of hydrogen in the mantle. To estimate the abundance of these compounds, one needs a greatly expanded solid-phase reaction set.

Last but not least, we offer our explanation to the observable “lack” of sulfur molecules in dark clouds (see e.g. Goicoechea et al. 2007, Wakelam et al. 2004, Palumbo et al. 1997). The calculated large abundance and n/MS of sulfur in highest oxidation state, namely SO_2 , in our model output allow us to suppose that the conditions within the mantles are suitable for many oxidized sulfur compounds that can essentially be described as derivatives of the sulfuric and sulfurous acids. These would include esters, sulfinic and sulfonic acids, sulfoxides, sulfones, peroxy-sulfuric acids, sulfamides, sulfimides, sulfamic acids, their derivatives and acid salts. Plenty of these molecules are known to be stable at 273K and should be durable in the mantles at 10K if they are able to form. Organic species include unsaturated thiols, thioethers and thioketones. Other species would be carbon disulfide CS_2 and those containing an S-S bond, already mentioned by Garozzo et al. (2010). Our idea is that a significant amount (say, some 40%) of sulfur is dissipated over a great variety of minor species (including many simpler radicals) and thus is hardly observable. An important assumption to explain why the derivatives are not observable in hot cores, is that when these species evaporate, they are reduced by hydrogen and dissociated in fragments by radiation. That is, these molecules lack gas production pathways. We suspect that a higher abundance of oxidized sulfur (mostly SO, SO_2 , CS) bearing species should be observable in the middle evolution stages of a hot core. Indeed, these observation results are presented, for example, by Mookerjee et al. (2007), Wakelam et al. (2003), Wakelam et al. (2004), Chandler et al. (2005), Jiménez-Serra et al. (2005) with abundances of SO_2 and, especially, SO typically larger than those of H_2S and comparable to OCS. A less well pronounced but similar effect can also be expected for the phosphorus family of compounds, as this element also is known to have a rich chemistry. One may argue that the “disappeared” sulfur in dark cores resides on grains in the form of oxides. This is however not confirmed by observations, e.g. Palumbo et al. (1997). It is well known that sulfur oxides tend to combine with water, which is thought to be the domi-

nant molecule on interstellar grains. In our opinion mantle sulfur chemistry can be expected to lead to the various acidic derivatives, besides other more conventional compounds. Some investigations of the sulfur chemistry (Palumbo et al. 1997, Ferrante et al. 2008) insist that the most important sulfur molecule known in dark cores OCS forms in water-deficient ices, so sulfur acid derivatives perhaps would be what one can expect from water-rich ices.

5. Conclusions

1. According to our model, which includes several basic assumptions (see Sect. 2), it is highly possible that chemical processes below the outer surface of interstellar grain mantles play an important role in the chemistry of dark molecular cloud cores.
2. An important factor that should be further investigated is the hydrogen diffusion through the grain mantles. This, combined with the continued dissociation of molecules by cosmic ray induced photons, leads to an overall outward flux of hydrogen from the mantle. According to our model results, the more dense the grain mantle, the more efficient is the outward diffusion of hydrogen. A more diverse, H-poor chemistry is encouraged below the surface, explaining the abundance of at least some species observed in dark molecular clouds and hot molecular cores.
3. A model based on the concept of pore surface reactions can at least partially describe the transformations occurring within the icy mantle.
4. Fe nuclei of cosmic-rays can be a cause of physical alteration of the mantle structure, but other possibilities, like light cosmic-ray particles, CR induced UV photons, and slow thermal diffusion may provide alteration with generally similar chemical consequences.
5. A combination of outer and inner mantle surface chemistry is able to produce a wide set of mantle species. It may ultimately lead to more accurate calculations of the composition of molecular clouds.
6. Further research is required to clarify many factors that are only approximately estimated. These include photodissociation and desorption yields, H and H_2 diffusion rate in amorphous dirty ices, the thickness of the mantle, the properties and number of the pores, reaction mechanism inside the grain mantles, effectiveness of selective desorption mechanisms, etc.
7. A chemically active and hydrogen poor environment in the mantle may explain the difficulties of observing sulfur in dark molecular cores. In grain mantles the rich chemistry of sulfur permits the formation of many various S molecules (mostly oxoacid derivatives) low on hydrogen, most of them with abundances too low to be observed. The large abundance of sulfur oxides in hot star-forming cores may be a direct consequence of these compounds being ejected into the gas phase.

References

- Aikawa, Y., Umebayashi, T., Nakano, T. & Miyama, S. M. 1997 *Ap.J.*, 486, L51
 Andersson, S. & van Dishoeck, E. F. 2008 *A&A*, 491, 907
 Awad, Z., Chigai, T., Kimura, Y., Shalabiea, O. M., Yamamoto, T. 2005 *Ap.J.*, 626, 262
 Baragiola, R. A., Bahr, D. A., Vidal, R. A. 2003 in *Astrophysics of Dust*, ed. A. N. Witt
 Brown, P. D., Charnley, S. B. 1990 *Mon. Not. R. Astron. Soc.*, 244, 432
 Chandler, C. J., Brogan, C. L., Shirley, Y. L., Loinard, L. 2005 *Ap.J.*, 632, 371

- Chang, Q., Cuppen, H. M., Herbst, E. 2007 A&A, 469, 973
Dalgarno, A. 2006 PNAS, 103, 12269
Das, A., Chakrabarti, S. K., Acharyya, K. & Chakrabarti, S. 2008 New Astron.,13, 457
Ferrante, R. F., Moore, M. H., Spiliotis, M. M., Hudson, R. L. 2008 Ap.J, 684, 1210
Freund, M. M., Freund, F. T. 2006 Ap.J, 639, 210
Garozzo, M., Fulvio, D., Kanuchova, Z., Palumbo, M. E., Strazzulla, G. 2010 A&A, 509, A67
Gerakines, P. A., Schutte, W. A., Ehrenfreund, P. 1996 A&A, 312, 289
Gerin, M. et al. 1997 A&A, 318, 579
Goicoechea, J. R., Pety, J., Gerin, M. et al. 2007 arXiv:astro-ph/0703393
Goldsmith, P. F., Li, D., Krčo, M. 2007 Ap.J, 654, 273
Hartquist, T. W., Williams, D. A. 1990 Mon. Not. R. Astron. Soc., 247, 343
Hasegawa, T. I., Herbst E., & Leung, C. E. 1992 Ap.J. Suppl. Ser., 82, 167
Hasegawa, T. I., Herbst, E. 1993a Mon. Not. R. Astron. Soc., 261, 83
Hasegawa, T. I., Herbst, E. 1993b Mon. Not. R. Astron. Soc., 263, 589
Hatchell, J., Thompson, M. A., Millar, T. J., MacDonald, G. H. 1998 A&A, 338, 713
Hollenbach, D., Kaufman, M. J., Bergin, E. A. & Melnick, G. J. 2009 Ap.J, 690, 1497
Jenkins, E. B. 2009 Ap.J, 700, 1299
Jiménez-Serra, I., Martín-Pintado, J., Rodríguez-Franco, A. & Martín, S. 2005 Ap.J, 627, L121
Mookerjee, B., Casper, E., Mundy, L. G., Looney, L. W. 2007 Ap. J, 659, 447
Nejad, L. A. M., Wagenblast R. 1999 A&A, 350, 204
Öberg, K. I., van Dishoeck, E. F. & Linnartz, H. 2009 A&A, 496, 281
Padovani, M., Galli, D., Glassgold, A. E. 2009 A&A, 501, 619
Palumbo, M. E., Geballe, T. R., Tielens, A. G. G. M. 1997 Ap.J, 479, 839
Roberts, J. F., Rawlings, J. M. C., Viti, S. & Williams, D. A. 2007 Mon. Not. R. Astron. Soc., 382, 733
Sánchez-Salcedo, F. J. & Vázquez-Semadeni, E. & Gazol, A. 2002 Ap.J, 577, 768
Schutte, W. A., Greenberg, J. M. 1991 A&A, 244, 190
Shalabiea, O. M., Greenberg, J. M. 1994 A&A, 290, 266
Strauss, H. L., Chen, Z., Loong, C.-K. 1994 J. Chem. Phys., 101, 7177
Tafalla, M., Myers, P. C., Caselli, P., Walmsley, C. M. 2004 A&A, 416, 191
Turner, B. E. 1998a Ap.J, 495, 804
Turner, B. E. 1998b Ap.J, 501, 731
Turner, B. E. 2000 Ap. J, 542, 837
van Weeren, R. J., Brinch, C., Hogerheijde, M. R. 2009 A&A, 497, 773
Wakelam, V., Castets, A., Ceccarelli, C. et al. 2004 A&A, 413, 609
Wakelam, V., Castets, C., Ceccarelli, C. et al. 2003 in proc. of conf. Chemistry as a Diagnostic of Star Formation, ed. C. L. Curry, M. Fich, 445
Widicus Weaver, S. L., Kelley, M. J., Blake, G. A. 2005 Proc. of the 231st Symp. of the IAU, 223
Willacy, K., Millar, T. J. 1998 Mon. Not. R. Astron. Soc., 298, 562
Willacy, K., Williams, D. A. 1993 Mon. Not. R. Astron. Soc., 260, 635
Woodall, J., Agúndez, M., Markwick-Kemper, A. J., Millar, T. J. 2006 A&A, 466, 1197

Table 4. Calculated gas phase fractional abundances of molecules.

Species	Abundance	Species	Abundance	Species	Abundance	Species	Abundance
H	8.39E-06	C7	1.21E-10	H2+	5.86E-14	N2+	4.80E-18
HE	1.67E-01	C7+	1.71E-18	H2C3H+	2.84E-13	N2O	0.00E+00
O	7.40E-08	C7H	9.39E-12	H2C5N+	5.31E-15	N2O+	0.00E+00
N	1.59E-08	C7H+	6.19E-16	H2C7N+	1.51E-16	NA+	5.24E-09
C	4.19E-09	C7H2	1.83E-11	H2C9N+	7.54E-18	NCCN	7.11E-09
MG	8.94E-08	C7H2+	2.21E-16	H2CCC	6.80E-10	NCCNCH3+	8.76E-20
S	1.56E-08	C7H3+	2.65E-16	H2CCCC	1.14E-10	NCCNH+	3.86E-14
SI	1.72E-08	C7H4	1.70E-14	H2CCO	4.00E-10	NH	2.41E-08
FE	1.24E-07	C7H4+	2.05E-18	H2CN	9.89E-12	NH+	4.85E-16
NA	3.60E-09	C7H5+	7.15E-19	H2CO	5.15E-08	NH2	7.00E-08
C10	5.15E-14	C7N	2.81E-12	H2CO+	5.87E-13	NH2+	5.84E-15
C10+	1.19E-18	C7N+	1.58E-24	H2CS	2.39E-09	NH2CN	1.48E-07
C2	1.39E-09	C8	7.76E-12	H2CS+	2.65E-14	NH2CNH+	8.63E-13
C2+	1.13E-17	C8+	1.51E-17	H2NC+	1.26E-13	NH3	5.97E-08
C2H	6.23E-09	C8H	6.24E-12	H2NO+	4.07E-13	NH3+	3.59E-12
C2H+	3.32E-17	C8H+	1.27E-19	H2O	2.05E-07	NH4+	2.26E-12
C2H2	3.37E-09	C8H2	1.66E-12	H2O+	1.11E-14	NO	6.82E-08
C2H2+	5.79E-15	C8H2+	1.71E-16	H2S	5.58E-09	NO+	5.38E-13
C2H3	1.54E-10	C8H3+	1.71E-17	H2S+	1.79E-13	NO2	5.80E-10
C2H3+	7.16E-14	C8H4+	6.59E-19	H2S2	3.22E-11	NO2+	1.87E-20
C2H3CN+	2.27E-23	C8H5+	1.02E-22	H2S2+	2.50E-15	NS	1.65E-09
C2H4	6.88E-09	C9	5.89E-12	H2SIO	2.20E-09	NS+	5.68E-14
C2H4+	1.70E-14	C9+	4.55E-19	H2SIO+	1.38E-14	O+	9.33E-16
C2H5	4.68E-09	C9H	4.63E-13	H3+	1.21E-09	O2	5.26E-08
C2H5+	3.06E-14	C9H+	3.29E-17	H3C3O+	2.42E-19	O2+	6.64E-14
C2H5OH	3.09E-13	C9H2	1.03E-12	H3C3OH3+	1.69E-20	O2H	3.30E-13
C2H5OH+	3.64E-18	C9H2+	1.14E-17	H3C3OH4+	3.82E-19	O2H+	2.60E-16
C2H5OH2+	6.39E-17	C9H3+	1.52E-17	H3C5N+	4.74E-21	OCN	2.51E-08
C2H7+	5.48E-21	C9H4+	2.95E-20	H3C7N+	7.73E-20	OCN+	2.66E-19
C2N	1.69E-10	C9H5+	4.50E-22	H3C9N+	6.50E-21	OCS	2.00E-10
C2N+	4.57E-14	C9N	1.28E-13	H3CO+	2.86E-12	OCS+	2.81E-16
C2N2+	1.64E-21	C9N+	8.39E-26	H3CS+	5.99E-14	OH	3.18E-07
C2NH+	5.92E-15	CH	5.98E-09	H3O+	2.74E-11	OH+	2.68E-15
C2O	1.41E-10	CH+	1.29E-16	H3S+	2.88E-13	S+	5.64E-11
C2O+	5.54E-16	CH2	6.24E-09	H3S2+	5.26E-15	S2	1.23E-09
C2S	3.88E-10	CH2+	4.24E-16	H3SIO+	7.84E-14	S2+	8.83E-15
C2S+	9.39E-19	CH2CHCN	1.86E-19	H4C3N+	2.85E-23	SI+	1.96E-10
C3	1.24E-09	CH2CN	5.92E-11	H5C2O2+	2.26E-20	SIC	5.77E-10
C3+	7.92E-17	CH2CN+	1.44E-15	HC2O+	1.51E-15	SIC+	1.05E-17
C3H	9.02E-10	H2CCO+	4.19E-16	HC2S+	1.01E-14	SIC2	1.38E-09
C3H+	6.74E-16	CH2NH	1.09E-08	HC3N	2.60E-10	SIC2+	8.79E-18
C3H2	1.99E-09	CH2NH2+	4.97E-15	HC3N+	5.17E-16	SIC2H	5.96E-10
C3H2+	5.77E-14	CH3	1.48E-08	HC3NH+	9.73E-15	SIC2H+	1.07E-13
C3H2O+	2.41E-21	CH3+	9.61E-13	HC3O+	1.15E-15	SIC2H2	1.34E-09
C3H3	2.51E-09	CH3C3N	9.30E-15	HC3S+	3.78E-15	SIC2H2+	2.80E-14
C3H3+	6.44E-14	CH3C3NH+	1.73E-18	HC4N+	1.44E-19	SIC2H3+	4.94E-14
C3H5+	1.05E-16	CH3C4H	2.76E-13	HC4S+	1.80E-17	SIC3	2.09E-10
C3H6+	2.30E-25	CH3C4H+	2.68E-18	HC5N	2.19E-11	SIC3+	6.35E-15
C3H7+	2.42E-22	CH3C5N	2.56E-16	HC5N+	8.46E-19	SIC3H	7.54E-11
C3N	1.55E-11	CH3C5NH+	1.16E-19	HC7N	2.20E-12	SIC3H+	1.72E-14
C3N+	1.78E-18	CH3C7N	2.53E-17	HC7N+	1.56E-17	SIC3H2+	9.68E-15
C3O	2.98E-11	CH3C7NH+	1.17E-20	HC9N	1.04E-13	SIC4	1.09E-14
C3O+	4.77E-20	CH3CCH	5.03E-10	HC9N+	7.17E-19	SIC4+	3.92E-15
C3S	8.99E-11	CH3CCH+	6.64E-15	HCN	2.97E-08	SIC4H+	1.47E-18
C3S+	1.05E-15	CH3CH3	7.85E-13	HCN+	4.31E-16	SICH2	8.53E-09
C4	7.28E-11	CH3CH3+	2.52E-14	HCNH+	5.90E-12	SICH2+	1.23E-13
C4+	3.27E-17	CH3CHO	9.17E-10	HCO	6.88E-09	SICH3	8.18E-13
C4H	1.35E-09	CH3CHO+	1.19E-14	HCO+	4.55E-12	SICH3+	7.51E-14
C4H+	9.11E-17	CH3CHOH+	1.28E-14	HCO2+	3.52E-14	SICH4+	2.41E-17
C4H2+	9.43E-14	CH3CN	2.45E-11	HCOOCH3	1.20E-16	SIH	5.85E-10
C4H3	1.18E-09	CH3CN+	2.95E-18	HCOOH	6.37E-13	SIH+	5.38E-13

Table 4. continued.

C4H3+	1.57E-15	CH3CNH+	1.29E-14	HCOOH+	5.42E-26	SIH2	3.53E-10
C4H4+	9.70E-15	CH3CO+	1.09E-14	HCOOH2+	6.76E-17	SIH2+	9.78E-15
C4H5+	1.39E-16	CH3COCH3	1.04E-15	HCS	5.03E-10	SIH3	3.12E-09
C4H7+	6.76E-20	CH3CS+	2.98E-16	HCS+	5.12E-14	SIH3+	6.38E-14
C4N	1.77E-10	CH3OCH3	1.35E-15	HCSI	6.95E-09	SIH4	5.22E-08
C4N+	4.72E-18	CH3OCH3+	1.13E-20	HCSI+	3.00E-17	SIH4+	2.99E-17
C4S	1.87E-13	CH3OCH4+	1.73E-19	HE+	6.38E-10	SIH5+	4.84E-13
C4S+	1.10E-15	CH3OH	1.84E-10	HEH+	1.02E-15	SIN	1.82E-09
C5	6.22E-10	CH3OH+	4.53E-16	HN2+	4.84E-14	SIN+	2.08E-13
C5+	6.18E-18	CH3OH2+	1.04E-15	HN2O+	0.00E+00	SINC+	4.95E-14
C5H	1.34E-10	CH4	5.04E-08	HNC	1.60E-08	SINH2+	2.63E-13
C5H+	8.34E-15	CH4+	1.92E-16	HNO	1.17E-08	SIO	9.20E-08
C5H2	3.96E-10	CH4N+	1.85E-15	HNO+	2.88E-13	SIO+	1.78E-15
C5H2+	1.26E-14	CH5+	1.37E-12	HNS+	8.05E-14	SIO2	2.35E-08
C5H3+	6.90E-15	CN	8.15E-09	HNSI	1.02E-08	SIOH+	4.97E-12
C5N	1.42E-11	CN+	2.58E-16	HNSI+	2.77E-17	SIS	1.71E-15
C5N+	2.13E-23	CNC+	7.26E-14	HOC+	9.55E-16	SIS+	2.19E-16
C6	1.18E-10	CO	2.95E-07	HS	6.52E-09	SO	1.20E-11
C6+	2.35E-17	CO+	3.45E-16	HS+	3.09E-13	SO+	2.35E-13
C6H	8.46E-11	CO2	2.10E-08	HS2	6.12E-11	SO2	1.65E-12
C6H+	8.34E-16	CO2+	2.03E-18	HS2+	7.71E-15	SO2+	2.73E-19
C6H2	3.26E-11	COOCH4+	1.47E-21	HSIO2+	1.83E-13	C+	5.39E-11
C6H2+	1.86E-15	CS	1.84E-09	HSIS+	7.94E-19	C5H5+	8.08E-18
C6H3+	3.20E-16	CS+	5.39E-17	HSO+	5.94E-16	C6H6	1.07E-12
C6H4+	1.05E-17	FE+	1.96E-07	HSO2+	5.49E-17	MG+	2.67E-08
C6H5+	1.46E-19	H+	2.21E-10	N+	1.22E-13	H2O2	5.94E-09
C6H6+	1.49E-16	H2	8.32E-01	N2	1.96E-08	E	2.33E-07
C6H7+	1.19E-17						